JOURNAL OF PROPULSION AND POWER
Vol. 36, No. 2, March–April 2020

Self-Excited Instability of Closed-Type Swirl Injector with Varying Conditions

Seokgyu Jeong* and Jinhyun Bae*
Seoul National University, Seoul 08826, Republic of Korea
Yunjae Chung†
Korea Aerospace Industries, Ltd., Daejeon 34068, Republic of Korea
Sam S. Yoon‡
Korea University, Seoul 02841, Republic of Korea
and
Youngbin Yoon§
Seoul National University, Seoul 08826, Republic of Korea

https://doi.org/10.2514/1.B37618

The dynamic characteristic of an injector is important for improving engine characteristics and preventing instability. In this study, the experiments on the unstable flow of a closed-type swirl injector were conducted, and the dynamic characteristic analysis of the relationship between internal and external flows was discussed. Consequently, it was found that the unstable characteristics of internal and external flows were similar. Main geometric parameters affecting the injector self-excited instability were also investigated. The fluctuating amplitude was mainly related to the momentum of the flow. On the other hand, the instability frequency was related to the axial velocity inside the swirl injector. Experiments with external pulsation were carried out to investigate the effect of the instability frequency in real environments. It was observed that the mean breakup length reduced by 25%, and the fluctuation amplitude of the spray angle increased more than twice compared with the out of tuned case. The results of this study can be an inspiration to engine design, considering the dynamic characteristics of an injector.

Nomenclature

A	=	area, mm^2
C	=	angular momentum constant, m^2/s
D	=	diameter, mm
D_H	=	hydraulic diameter, mm
f	=	frequency, Hz
K	=	injector geometric constant
k	=	wave number
L	=	length, mm
$\dot{m}$	=	mass flow rate, g/s
N_t	=	number of tangential inlets
R	=	inflow radius, mm
U	=	flow velocity, m/s
α	=	reflection coefficient
α_c	=	swirl chamber converging angle, deg
ε	=	orifice filling coefficient
θ	=	spray half angle, deg
ξ	=	wave position, mm
ρ	=	water density, kg/m^3
Ω	=	surface wave amplitude
ω	=	angular disturbance frequency with stationary condition

Subscripts

a	=	air core
ax	=	axial
in	=	injector inlet
o	=	orifice
t	=	tangential inlet port
tan	=	tangential
s	=	swirl chamber

Received 3 April 2019; revision received 14 October 2019; accepted for publication 22 October 2019; published online 23 November 2019.

*Ph.D. Candidate, Department of Mechanical and Aerospace Engineering.
†Research Engineer, Satellite Development Department.
‡Professor, School of Mechanical Engineering.
§Professor, Department of Mechanical and Aerospace Engineering, Institute of Advanced Aerospace Technology; ybyoon@snu.ac.kr (Corresponding Author).

I. Introduction

THERE have been many developments in the space launch vehicle industry, and there has been increasing interest in manned launch vehicle projects such as space tourism and space station business. As a result, the stability of a rocket launch vehicle has become more important. One of the most dangerous instabilities of a launch vehicle is the combustion instability of the engine. To solve the combustion instability, baffle or acoustic cavities are generally used. However, these methods decrease the payload mass of the launch vehicle owing to the additional mass on engine structure. The method of changing the dynamic characteristics of an injector of a launch vehicle has the advantage that it does not have a great influence on the engine efficiency because no additional mass is added.

In general, the propulsion system consists of three parts: feedline, injector, and combustion chamber. A schematic of the dynamic process of the system is shown in Fig. 1 [1,2]. When the pressure perturbation occurs during the combustion process, it affects the combustion chamber and the velocity fluctuation of the injector. The generated velocity perturbation affects the pressure difference perturbation of the feed system, which in turn influences the velocity perturbation of the injector. If the perturbation of the entire system operates with positive feedback, the instability increases, thereby causing failure. As the injector serves as an intermediate bridge for the entire system, it is possible to control the entire instability by changing the injector based on a suitable design.

Owing to this feature, many research studies on the characteristics of an injector have been carried out by various groups. They focused not only on the static characteristics such as the spray angle and liquid film thickness of an injector, but also on its dynamic characteristics such as the injector transfer function. Bazarov established the injector dynamics theory and defined the injector transfer function as the output flow divided by the input pressure [1]. Ismailov and Heister

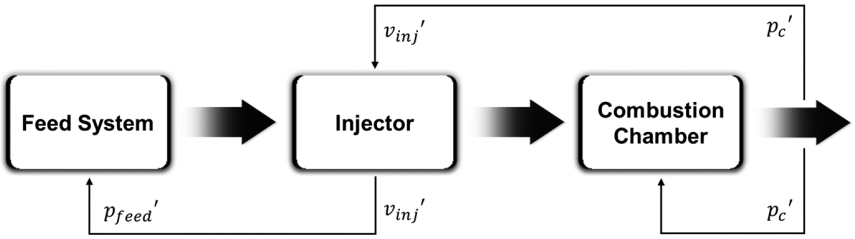

Fig. 1 Scheme of dynamic process interaction in the propulsion system [1,2].

theoretically and numerically studied the resonance phenomenon caused by the surface wave generated inside a closed-type swirl injector [3,4]. Chen and Yang numerically analyzed the flow characteristics of a swirl injector according to the changes in the atmospheric pressure conditions, and analyzed the unstable phenomenon occurring inside the injector [5]. These studies showed that the instability of the swirl injector flow is largely related to the internal flow characteristics, and some groups carried out experimental studies on the flow characteristics of a swirl injector using a high-speed backlight imaging technique to confirm its air core characteristics [6,7]. In the case of a swirl injector, the external flow develops into a thin liquid sheet. Dombrowski and Johns showed that wavy flow occurs owing to aerodynamic forces acting on a thin liquid sheet [8]. Lienemann et al. experimentally confirmed the phenomena occurring in the attenuating liquid sheet [9].

It is known that the atomization instability of an injector is closely related to combustion instability. Anderson et al. confirmed that the atomization frequency in an impinging jet injector is related to the frequency of combustion instability [10]. Ahn and Choi experimentally confirmed the importance of injector dynamics. By comparing the frequency of combustion instability to the instability frequency calculated from the injector dynamics, they suggested that the characteristics of injector dynamics might be related to the actual combustion instability [11]. In addition, a few groups performed experimental studies by using an external pulsating device to find more detailed characteristics of the injector transfer function in real situations [12–16].

However, the experimental results on self-instability of swirl injector flow are still insufficient. Therefore, the internal and external flows of a swirl injector with self-unstable condition were experimentally investigated in this study. Through experiments of unstable characteristics with changing pressure and injector structure, data of unstable flows generated in thin liquid sheets with tangential velocity were acquired, and the parameters affecting dynamic characteristics of this type of sheet flow were examined. Furthermore, an external pulsation test was performed to investigate the effect of instability in actual environments.

II. Experimental Methods

A. Experimental Apparatus

Figure 2 shows the schematic diagram of the closed-type swirl injector used in this study. Water was used as the experimental fluid. The manifold pressure before the tangential inlets was measured as the pressure difference of the injector was obtained using a static pressure sensor (Valcom, VPRQ-A5-20Bar-4C, uncertainty $= \pm 0.8\%$) and controlled by a regulator (accuracy $= \pm 0.02$ atm). The liquid flow rate was measured using a flow meter (Hoffer Flow Control, HO1/2X1/4A-.35-3.5-BP-1MX-MS-X, uncertainty $= \pm 0.49\%$) that was installed at the feed line. The base geometry of the swirl injector was as follows: the swirl chamber length L_s was 19 mm, swirl chamber diameter D_s was 18 mm, orifice diameter D_o was 6 mm, number of tangential inlet port N_t was 3, and tangential inlet port diameter D_t was 1 mm. As shown in Table 1, experiments were carried out using various structures to study the geometric effect on the dynamic characteristics of the swirl injector. In addition, pressure difference between the injector and ambient air was varied from 1 to 7 atm to find the effect of the flow rate. The ambient pressure was fixed at 1 atm. Under these conditions, an image of the spray flow was taken by using a backlight image technique using a high-speed camera (Photron, FASTCAM-ultima APX) at 6000 frames per second and continuous light source (Photron, HVC-SL). As the images of internal and external spray flows had to be taken, injectors were made of a transparent acrylic material. At this time, the frame resolution was set at 1024×1024 pixels for external image and at 512×512 pixels for internal image. Furthermore, a hydraulic pulsator used in previous work [15] was installed before the injector to apply pressure perturbation. This type of pulsator was most suitable in this study because it could provide strong pulsation in high-momentum fluids than other pulsators [17].

B. External Flow Image Analysis

From the external spray images, the flow was either stable or unstable depending on the geometry of the swirl injector, as shown in the Fig. 3. When the instability occurred, the spray fluctuated more dynamically, and the average breakup length decreased versus the stable condition. To confirm this instability phenomenon more precisely, a high-speed imaging technique was used. The analysis process used in this study is shown in Fig. 4. Figure 4a shows one of the raw images. The binarization of the original image was carried out to determine the surface of the external spray. Images with distinct surfaces were then taken, as shown in Fig. 4b. The spray angle was calculated from four points of the image: both ends of the injector tip and both ends of surface points, which were 6 mm below the injector tip. When the same process was applied to the entire image, the time

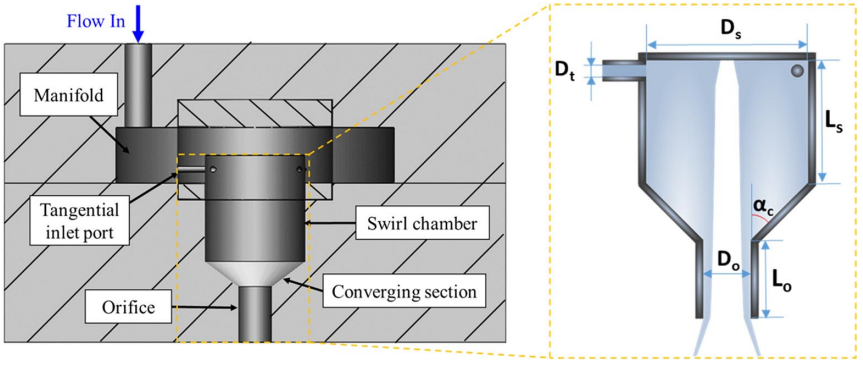

Fig. 2 Schematic of closed-type swirl injector.

Table 1 Injector geometry

Parameter	Dimension
Number of tangential inlets, N_t	2, 3, 4, 5
Inlet port diameter, D_t, mm	1, 2, 3
Swirl chamber length, L_s, mm	19, 24, 28
Swirl chamber diameter, D_s, mm	18, 21
Orifice length, L_o, mm	10
Orifice diameter, D_o, mm	6, 9
Converging angle, α_c, °	45

domain spray angle graph, shown in Fig. 4c, was obtained, and it was found that the fluctuation amplitude was strong within a specific frequency range. Waterfall Fast Fourier Transform (FFT) was performed at intervals of approximately 0.04 s as shown in Fig. 5 to confirm the change in fluctuation frequency and calculate the mean fluctuation frequency. The peak frequency of each sample and calculated mean fluctuation frequency are listed in Table 2.

C. Internal Flow Image Analysis

Flow oscillating factors such as film hydrodynamics and swirl postacoustics exist inside a swirl injector [18]. To understand the cause of the instability, it was necessary to investigate the phenomenon inside the injector. Therefore, the image of the internal flow of the swirl chamber, as shown in Fig. 6, was taken using the backlight technique. During this time, the light intensity exhibited a unique profile, showing a distinct boundary of intensity at particular locations. This profile was similar to Kenny's film thickness image. Kenny explained that the intensity derivative is either minimum or maximum at locations where the nozzle diameter edge distorted the background light [7]. Using this information, the air core diameter, indicated by red arrows in Fig. 6, was obtained.

To find the dynamic characteristics, an analysis process, shown in Fig. 7, was carried out in a manner similar to the external spray case. First, the points before the swirl chamber converging section, indicated by the red arrows in Fig. 7b, were chosen, and the air core diameter was calculated from the image. Next, 6000-fps images were used to get the time domain air core diameter graph. To determine the dynamic characteristics, the waterfall FFT process was performed, and the mean fluctuation frequency of internal flow was also obtained

III. Results and Discussion

A. External and Internal Flow Dynamic Characteristics

Based on this, the mean frequency of self-excited instability of the external spray angle and internal flow were measured by changing the mass flow rate under the conditions of swirl chamber diameter of

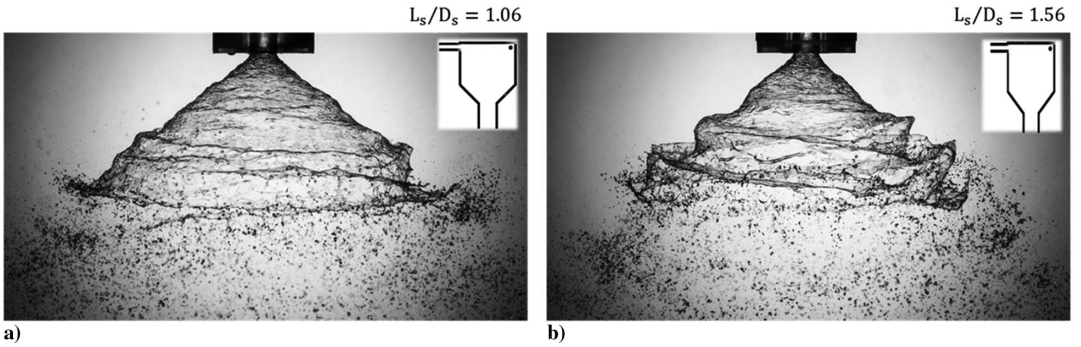

Fig. 3 External spray image of a) stable and b) unstable conditions.

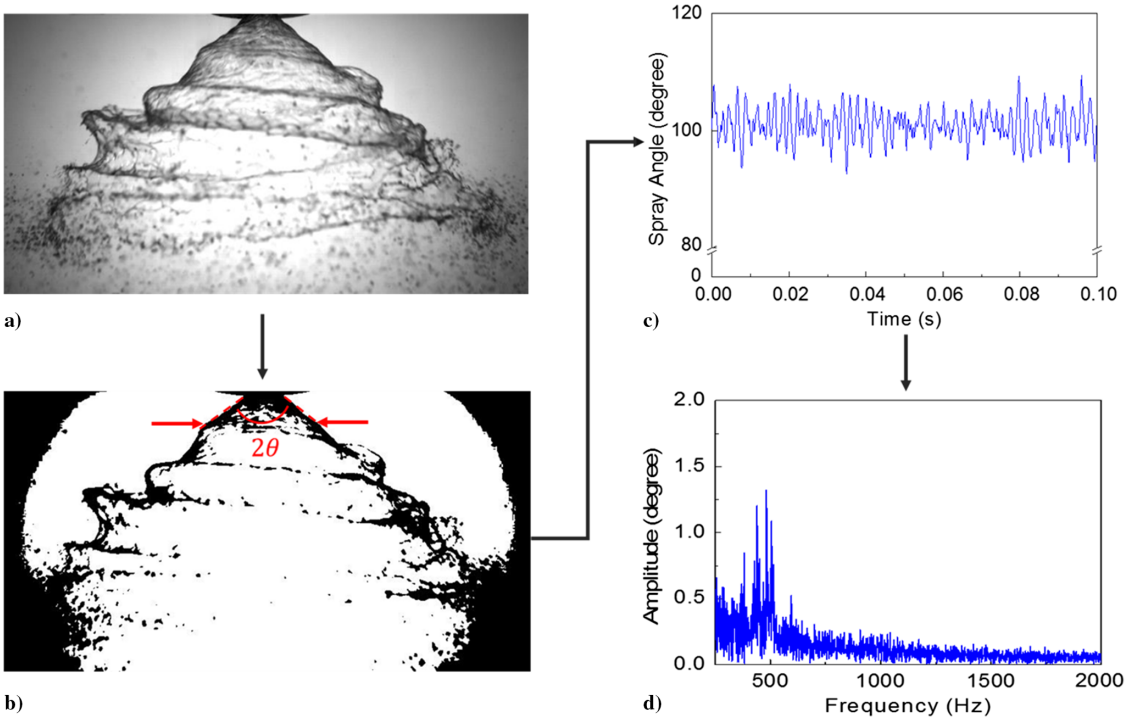

Fig. 4 Dynamic analysis process of external spray: a) raw image, b) binarization, c) spray angle with time, and d) FFT result.

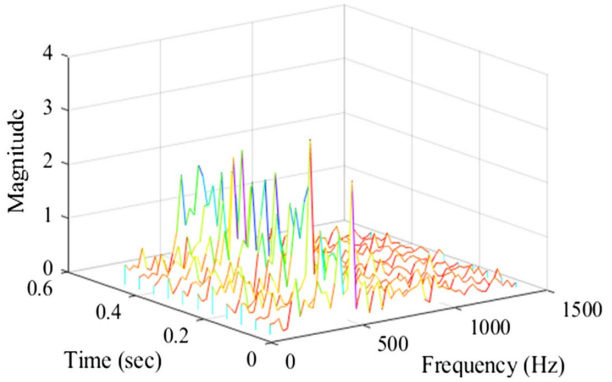

Fig. 5 Waterfall FFT result of external spray.

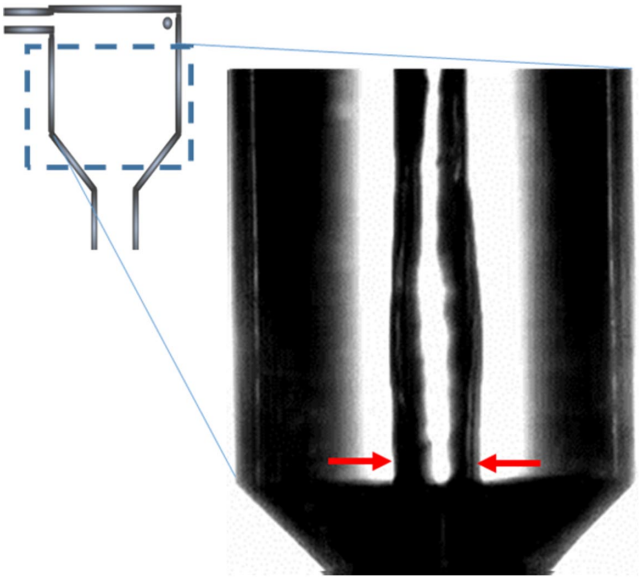

Fig. 6 Backlight image of swirl chamber internal flow.

19 mm and swirl chamber length of 28 mm, which showed an unstable spray. Figure 8a shows the amplitude with mass flow rate obtained from the time domain spray angle graph for external spray, and from the time domain air core diameter graph for internal flow. During this time, the amplitude was calculated from the normalized root mean square (RMS) deviation value, as expressed in Eq. (1).

$$\mathrm{Amp}_{\mathrm{external}} = \frac{\sqrt{\sum_{i=1}^{n}(2\theta_i - 2\theta_{\mathrm{mean}})^2}}{2\theta_{\mathrm{mean}}}$$

$$\mathrm{Amp}_{\mathrm{internal}} = \frac{\sqrt{\sum_{i=1}^{n}(D_{a,i} - D_{a,\mathrm{mean}})^2}}{D_{a,\mathrm{mean}}} \tag{1}$$

For sinusoidal waves, peak-to-peak amplitude is proportional to the RMS value. Hence, the amplitude could be compared using the above equation. Consequently, it was confirmed that the fluctuating amplitude decreased slightly with increasing mass flow rate for external and internal flow cases. It was also confirmed that the mean fluctuation frequency increased proportionally with increasing flow rate for external and internal flow cases, as shown in Fig. 8b. It can be observed from this graph that the unstable characteristic of the external spray is similar to that of internal flow. Consequently, it can be seen that the instability characteristics of the external spray and the internal flow are due to the same causes. To the next, experiments with various injector geometries were carried out for more detailed analysis about the self-excited instability of the injector. At this time, because the dynamic characteristics of the internal and external flow were almost the same, only air core diameter was measured.

B. Main Parameters Affecting Self-Excited Instability Frequency

First, the swirl chamber geometry was varied. Figure 9 shows the injector self-excited instability characteristics with mass flow rate changing the swirl chamber length to 19, 24, and 28 mm. It can be seen that the swirl chamber length has no effect on mean fluctuation frequencies; however, it significantly affects the fluctuating amplitude. As the swirl chamber length increased, the fluctuating amplitude became larger. Figure 10 shows the injector self-excited characteristics with mass flow rate changing the swirl chamber diameter to 18 and 21 mm. It can be seen that the swirl chamber diameter also has no effect on self-excited frequencies but affects the fluctuating amplitude to some extent. As the swirl chamber diameter increased, the fluctuating amplitude became smaller. Consequently, it was found that, as the swirl chamber length to diameter ratio increased, the flow became more unstable. This phenomenon was also presented in a previous study of Kim et al. [6], and they confirmed that the flow instability occurs owing to the axial friction at the injector wall, which increases as the swirl chamber length-to-diameter ratio increases.

Table 2 The peak frequency of each sample and mean fluctuation frequency from waterfall FFT

Time, s	Frequency, Hz
0–0.043	515.625
0.043–0.085	421.875
0.085–0.128	445.313
0.128–0.171	515.625
0.171–0.213	492.188
0.213–0.256	492.188
0.256–0.299	445.313
0.299–0.341	468.750
0.341–0.384	492.188
0.384–0.427	515.625
0.427–0.469	468.750
Mean frequency: 479.404 Hz	

Next, the influence of the inlet geometries on instability was examined. Figure 11 shows the results with changing the tangential inlet port diameter to 1, 2, and 3 mm. Figure 11a shows that the fluctuating amplitude decreases slightly as the mass flow rate increases and inlet port diameter decreases. Figure 11b shows that the mean fluctuation frequency varies unlike the swirl chamber case. The frequency decreases as the inlet port diameter increases. Figure 12 shows the results with mass flow rate changing the numbers of tangential inlet ports to 2, 3, 4, and 5. It can be seen that there is no clear relation between the numbers of inlet ports and fluctuating amplitude; however, the mean fluctuation frequency decreases as the number of inlet ports increases. Consequently, it was found that the mean fluctuation frequency was inversely proportional to the swirl injector inlet area A_{in}.

The influence of the outlet geometry was also examined. Figure 13 shows the results with mass flow rate changing the orifice diameter to 6 and 9 mm. It can be seen that the fluctuating amplitude does not change significantly, similar to the number of inlet port case. However, the mean fluctuation frequency decreases as the orifice diameter increases, which means increase in the injector outlet area A_{out}.

In summary, components such as mass flow rate, swirl chamber length and diameter, and tangential inlet port diameter were found to have effect on the fluctuating amplitude. These components had one thing in common that they all were related to the angular momentum of the swirl injector. The angular momentum constant can be expressed as shown in Eq. (2).

$$C = U_{\mathrm{in}}R = \frac{1}{2}U_{\mathrm{in}}(D_s - D_t) = U_{\tan}R_a \tag{2}$$

In the experimental results presented in this paper, the angular momentum constant decreased as the fluctuation amplitude increased: As the mass flow increases and the tangential inlet port diameter

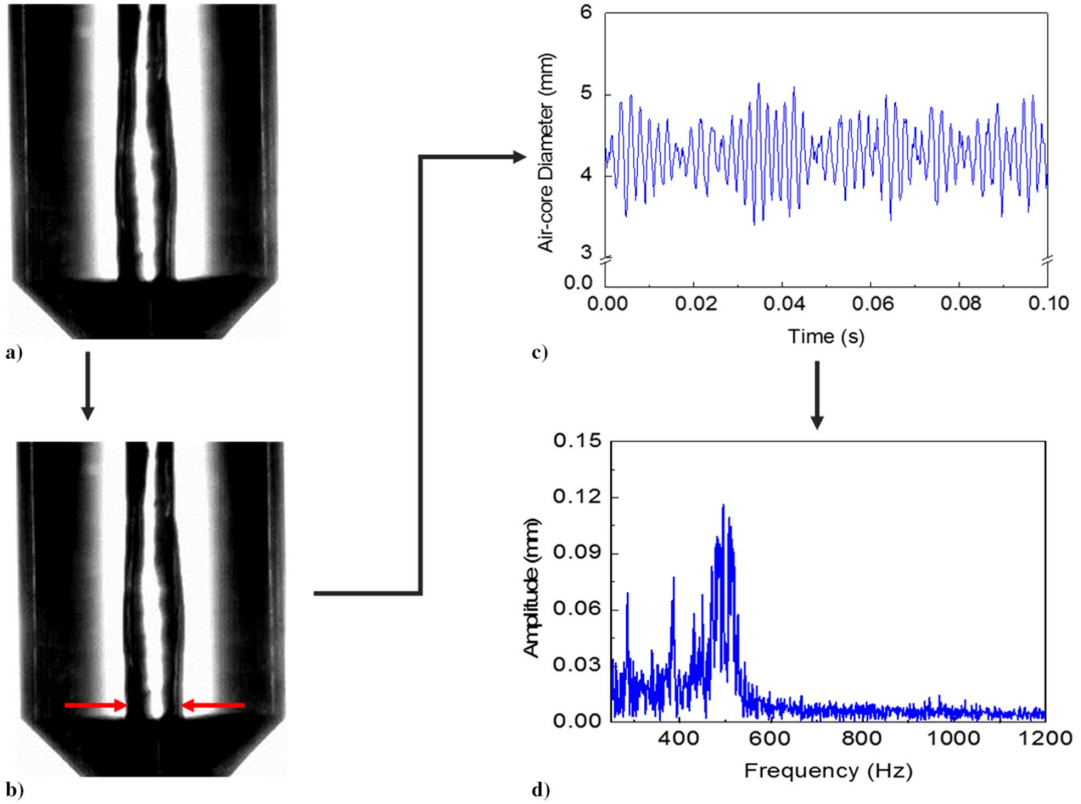

Fig. 7 Dynamic analysis process of internal flow: a) raw image, b) measuring point, c) air core diameter with time, and d) FFT result.

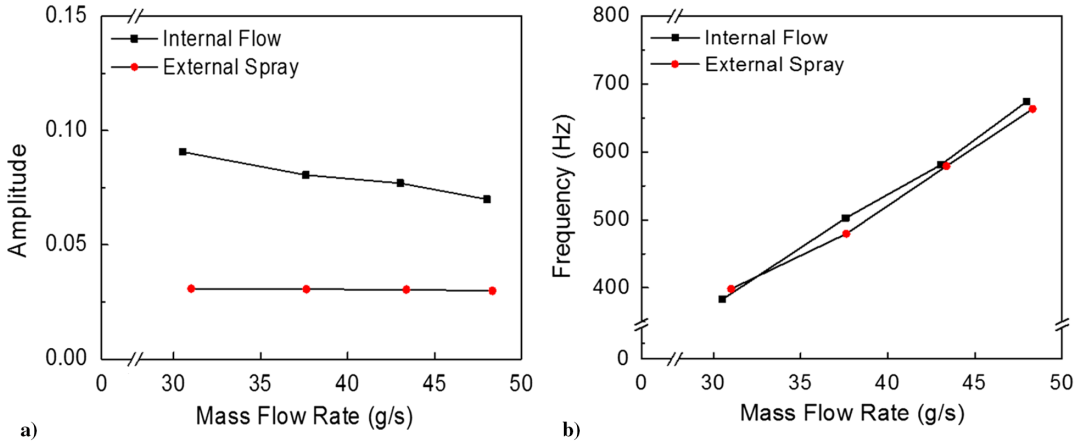

Fig. 8 External spray angle and internal air core diameter a) fluctuation amplitude and b) frequency with mass flow rate at $L_s = 28$ mm case.

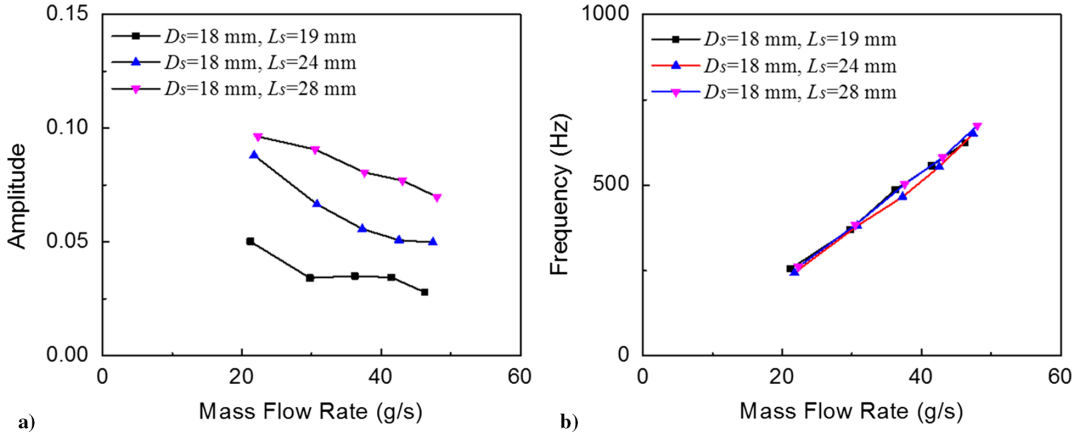

Fig. 9 a) Injector self-excited instability amplitude and b) frequency with mass flow rate varying swirl chamber length to 19, 24, and 28 mm.

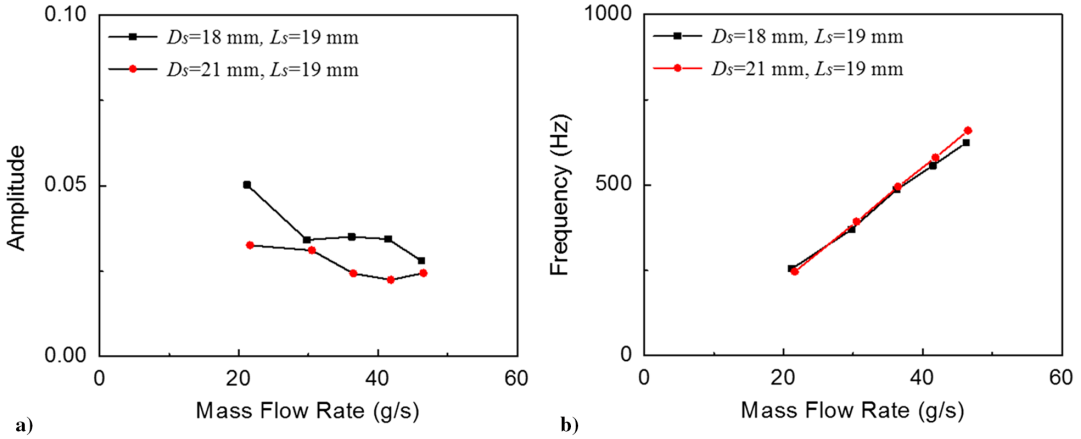

Fig. 10 a) Injector self-excited instability amplitude and b) frequency with mass flow rate varying swirl chamber diameter to 18 and 21 mm.

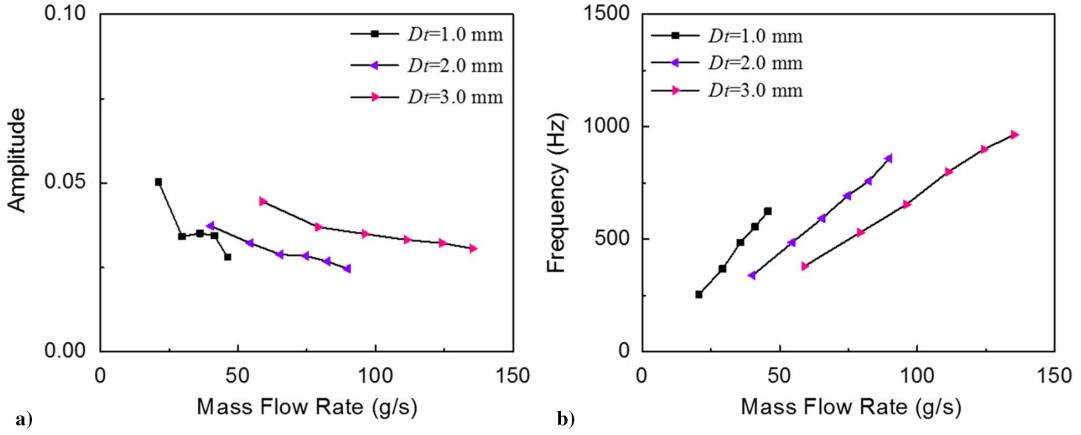

Fig. 11 a) Injector self-excited instability amplitude and b) frequency with mass flow rate varying tangential inlet port diameter to 1, 2, and 3 mm.

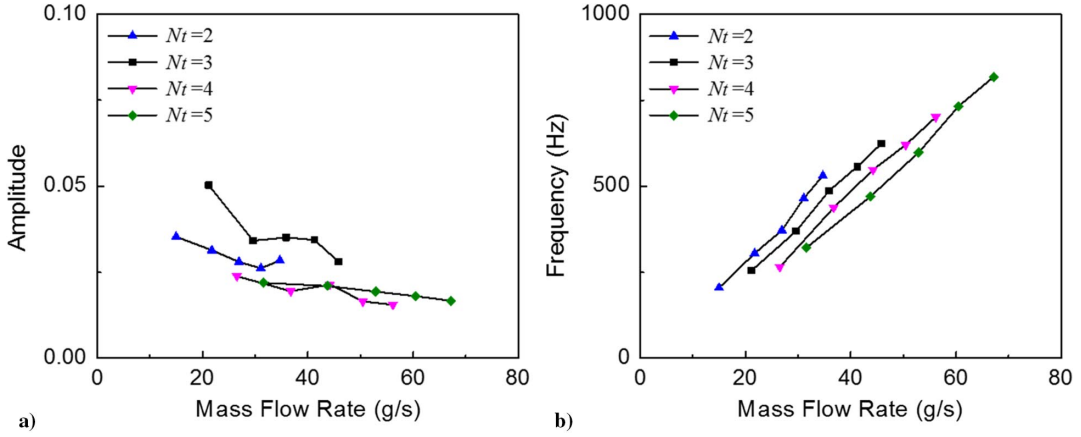

Fig. 12 a) Injector self-excited instability amplitude and b) frequency with mass flow rate varying number of tangential inlet ports to 2, 3, 4, and 5.

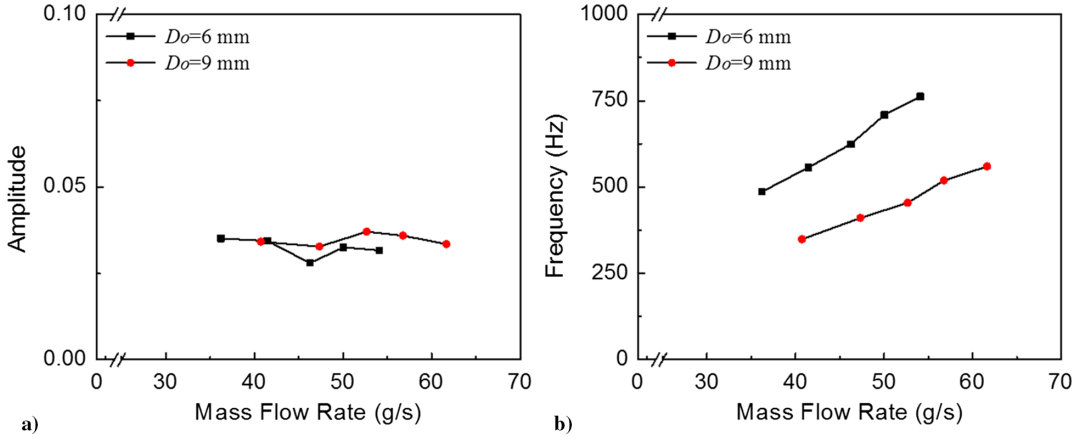

Fig. 13 a) Injector self-excited instability amplitude and b) frequency with mass flow rate varying orifice diameter to 6 and 9 mm.

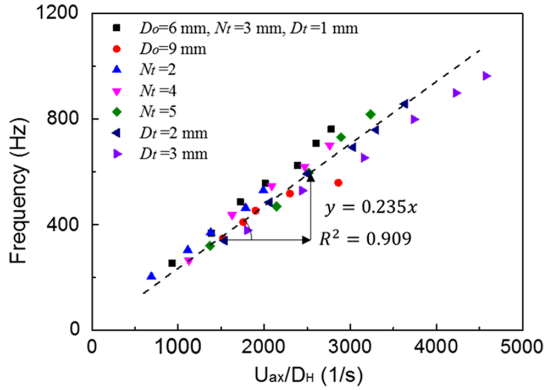

Fig. 14 Injector self-excited instability frequencies with axial velocities divided by hydraulic diameters at orifice for all experimental cases.

decreases, the inlet velocity increases. As the swirl chamber diameter increases, the angular momentum increases. As the swirl chamber length increases, the angular momentum at the orifice exit reduces more because of wall friction. The tangential velocity of the sheet flow increases with increasing angular momentum; that is, high tangential velocity affects stable flow.

In addition, three more components, mass flow rate, inlet area A_{in}, and outlet area A_o, were found to have effect on the mean fluctuation frequency. These three components had one thing in common that they were related to the axial velocity of swirl injector. The axial velocity of swirl injector can be expressed as shown in Eq. (3).

$$U_{\text{ax}} = \frac{m}{\rho(A_o - A_a)} \tag{3}$$

From Eq. (3), it can be easily found that the axial velocity is proportional to the mass flow rate and inversely proportional to the orifice area. The relationship between the inlet area and the axial velocity can be explained using several relations.

$$K = \frac{\pi R d_o}{2N_t A_t} \tag{4}$$

$$\epsilon = \frac{A_e}{A_o} = \frac{A_o - A_a}{A_o} = 1 - \frac{A_a}{A_o} \tag{5}$$

$$K = \frac{(1-\epsilon)\sqrt{2}}{\epsilon\sqrt{\epsilon}} \tag{6}$$

When inlet area increases, the injector geometric constant K, defined in Eq. (4), decreases. Using the maximum flow principle in swirl injector, the relation between the injector geometric constant and orifice filling coefficient ϵ is expressed in Eq. (6) [19]. To sum up, the orifice filling coefficient increases as the inlet area increases, and by referring to the definition of the orifice filling coefficient, expressed in Eq. (5), as the air core sectional area increases, the axial velocity decreases. This means that axial velocity is inversely proportional to the inlet area. Supposing that the injector self-excited instability frequency is proportional to the axial velocity, the trends observed in the experimental results can be explained. To obtain a precise verification, axial velocities were obtained by substituting the air core diameter, determined from the experimental image, into Eq. (3). The mean fluctuation frequencies with axial velocities for all experimental cases are shown in Fig. 14. During this time, the axial velocity was divided by the hydraulic diameter D_H $(= D_o - D_a)$ at orifice to make its unit the same as frequency. Consequently, it was found that the mean fluctuation frequency was proportional to the axial velocity of the swirl injector. In addition, the slope, which was expressed in the same way as Strouhal number in Eq. (7), remained constant at a value of approximately 0.235 for these study cases.

$$\text{Slope} = \frac{fD_H}{U_{\text{ax}}} \tag{7}$$

More detailed analysis of the self-excited instability is discussed in next section.

C. Discussion on Self-Excited Instability

There are various causes of swirl injector self-excited instability, such as surface wave resonance and unstable sheet by the aerodynamic or hydrodynamic force generated in the injector. In the case of self-excited instability in this study, even if the length and diameter of the swirl chamber changed, there were no changes in unstable frequency as shown in Figs. 9 and 10. This result indicates that the self-excited instability may be caused by the external sheet instability rather than the internal wave resonance effect in the swirl chamber. The experimental results show that the flow characteristics were similar to the preferred mode of thin liquid sheet owing to aerodynamic force. According to Dombrowski and Johns [8], the thin liquid sheet flow develops as wavy flow caused by the influence of the pressure force, surface tension force, inertial force, and shearing force. The increase in main frequency owing to the increase in flow velocity observed in this study is caused by an increase in the wave velocity as the external flow velocity increases. This result is confirmed by Lienemann et al.'s attenuating liquid sheet test [9].

In the case of the external flow of the swirl injector in this study, there existed a tangential velocity term unlike the general fan-sheet flow. The tangential velocity did not affect the axial wave frequency of the sheet, but it affected the total liquid momentum. As the tangential velocity increased, the flow became robust to external disturbance. In the study of Im et al. [20], although a gas–liquid swirl coaxial injector was used, it was confirmed that as the liquid momentum increases in the sheet-type spray, the resistance to disturbance due to air flow increases. In addition, self-excited instability decreases as the liquid momentum increases in the sheet-type spray. The next section will discuss the importance of this mean fluctuation frequency.

D. Effect of External Perturbation with Mean Fluctuation Frequency

To investigate the effect of mean fluctuation frequency in real situations, experiments with external perturbation were carried out using a mechanical pulsator. A relatively stable injector geometry, the

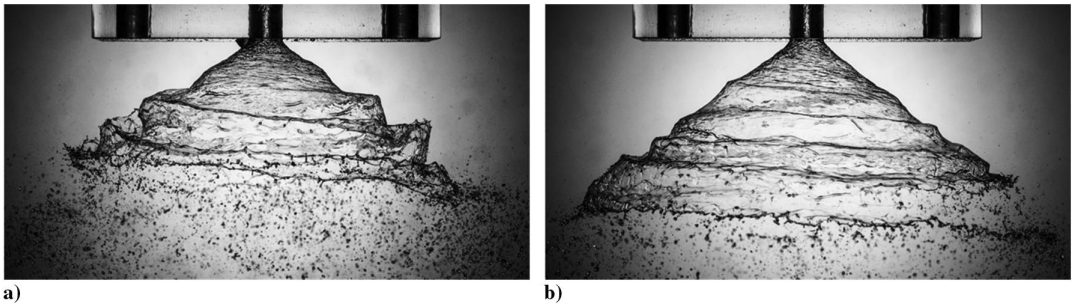

a) b)

Fig. 15 External spray images with external perturbation of a) tuned (312 Hz) and b) out-of-tune (350 Hz) cases.

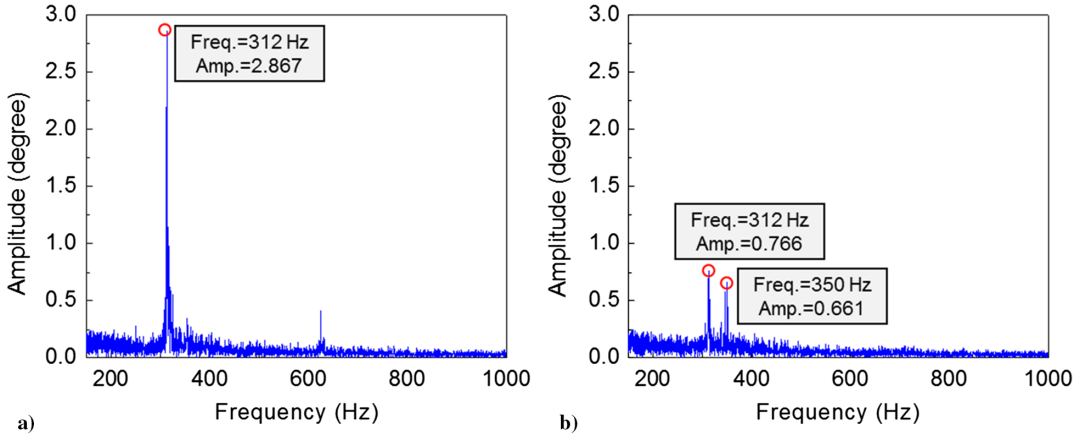

Fig. 16 FFT results of external spray angle with external perturbation for a) tuned (312 Hz) and b) out-of-tune (350 Hz) cases.

swirl chamber of diameter 18 mm, swirl chamber of length 19 mm, three tangential entries, tangential entry of diameter 1 mm, and orifice of diameter 9 mm were selected, and the mean fluctuation frequency was set as 312 Hz. For comparison, external pulsations of 312 and 350 Hz were applied for tuned and out-of-tune cases. Significant differences can be observed between two spray images with external pulsation, as shown in Fig. 15. First, the mean breakup length observed in the tuned case is 34.6 mm, which is 25% shorter than the mean breakup length in out of tune case, which is 46.7 mm. The breakup length is one of the important factors determining the size of the combustion chamber. If the breakup length is greater than the design value, there is a problem that the spray or flame reaches the wall of the combustion chamber, and if the breakup length is shorter than the designed value, it becomes difficult to mix the propellant sufficiently [21]. According to the results of this study, it can be observed that the breakup length can be changed even when the structure and pressure difference are the same.

Furthermore, the strength of the fluctuation was high in the tuned case. Figure 16 shows the FFT results of external spray angle with external perturbation for tuned and out-of-tune cases. Figure 16a shows only one peak frequency at 312 Hz for the tuned case, and Fig. 16b shows two peak frequencies, the mean fluctuation frequency at 312 Hz and the applied frequency at 350 Hz, for the out-of-tune case. In the out-of-tune case, the FFT amplitude, which means the strength of the fluctuation, at 312 Hz was 0.766° and the FFT amplitude at 350 Hz was 0.661°, which was excited to a similar strength as in the case of mean fluctuation frequency. However, when these two perturbation strengths were applied with the same frequency, the FFT amplitude changed to 2.867°, which was 2.01 times higher than the simple addition of natural and applied amplitudes. When the spray angle fluctuation increases, the engine efficiency can decrease because some of the propellants reach the combustion chamber wall. To solve this problem, it is not only necessary to design an injector with low fluctuation amplitude, but also important to check the frequency band of external sources and avoid this frequency band by considering the self-excited instability of injector.

IV. Conclusions

The external spray characteristics of a closed-type swirl injector were investigated, and it was confirmed that the closed-type swirl injector could be unstable when the value of the swirl chamber length-to-diameter ratio was high. This type of instability was defined as the self-excited instability of swirl injector, and the spray angle fluctuation amplitude and mean frequency were used to analyze this instability. The amplitude was obtained from the RMS value of the time domain spray angle graph, and the frequency was determined from the mean of waterfall FFT peak frequencies. Next, it was found that the self-excited instability frequency was proportional to the mass flow rate, and amplitude decreased slightly as the mass flow rate increased. To find the cause of this instability, the internal flow characteristics were also investigated using the high-speed back light images of the swirl chamber, and the air core diameter fluctuation amplitude and frequency were used to analyze the internal flow instability. Consequently, it was found that the unstable characteristics of internal and external flows were similar, which indicated that the cause of external and internal instability was same.

Main geometric parameters affecting the injector self-excited instability were also investigated. The fluctuation amplitude was mainly related to the swirl chamber length-to-diameter ratio, which was related to the angular momentum and wall friction. On the contrary, the mean fluctuation frequency was related to the mass flow rate, tangential inlet area, and orifice area, which were related to the axial velocity inside the swirl injector. The linear relation between mean fluctuation frequency and axial velocity was confirmed by the preferred mode theory of liquid sheet.

Experiments with external pulsation were carried out to investigate the effect of mean fluctuation frequencies in real situations. Consequently, it was found that the spray characteristic changed greatly when the external perturbation with the same frequency as the mean fluctuation frequency was applied. The breakup length reduced by 25% compared with that of the general perturbation case, and the fluctuation amplitude of the spray angle increased more than twice. If the spray characteristics are different from those when the engine is designed, problems such as the spray reaching the combustion chamber walls or reduced mixing characteristics can occur, which can reduce the engine efficiency. Therefore, it is important to study the dynamic characteristics of the injector to avoid such instabilities. The results of this study indicate a simple example of the injector dynamic phenomenon and are expected to help in the injector designing, considering their dynamic characteristics. In addition to these results, if spray properties related to combustion such as droplet size and experimental results with real propellants are investigated, it is expected that the effect on combustion instability can be confirmed.

Acknowledgments

This work was supported by Advanced Research Center Program (NRF-2013R1A5A1073861) through the National Research Foundation of Korea (NRF) grant funded by the Korean government Ministry of Science and ICT (MSIP) contracted through Advanced Space Propulsion Research Center at Seoul National University, and by the Korean government (NRF-2016-Fostering Core Leaders of the Future Basic Science Program/Global Ph.D. Fellowship Program).

References

[1] Bazarov, V. G., *Liquid Injector Dynamics*, Mashinostroenie, Moscow, 1979, Chaps. 1, 3, 4.

[2] Bazarov, V. G., and Yang, V., "Liquid-Propellant Rocket Engine Injector Dynamics," *Journal of Propulsion and Power*, Vol. 14, No. 5, 1998, pp. 797–806. https://doi.org/10.2514/2.5343

[3] Ismailov, M., and Heister, S. D., "Dynamic Response of Rocket Swirl Injectors, Part I: Wave Reflection and Resonance," *Journal of Propul-*

sion and Power, Vol. 27, No. 2, 2011, pp. 402–411.
https://doi.org/10.2514/1.B34044
[4] Ismailov, M., and Heister, S. D., "Dynamic Response of Rocket Swirl Injectors, Part II: Nonlinear Dynamic Response," *Journal of Propulsion and Power*, Vol. 27, No. 2, 2011, pp. 412–421.
https://doi.org/10.2514/1.B34045
[5] Chen, X., and Yang, V., "Effect of Ambient Pressure on Liquid Swirl Injector Flow Dynamics," *Physics of Fluids*, Vol. 26, No. 10, 2014, Paper 102104.
https://doi.org/10.1063/1.4899261
[6] Kim, S., Khil, T., Kim, D., and Yoon, Y., "Effect of Geometric Parameters on the Liquid Film Thickness and Air Core Formation in a Swirl Injector," *Measurement Science and Technology*, Vol. 20, No. 1, 2008, Paper 015403.
https://doi.org/10.1088/0957-0233/20/1/015403
[7] Kenny, R. J., Hulka, J. R., Moser, M. D., and Rhys, N. O., "Effect of Chamber Backpressure on Swirl Injector Fluid Mechanics," *Journal of Propulsion and Power*, Vol. 25, No. 4, 2009, pp. 902–913.
https://doi.org/10.2514/1.38537
[8] Dombrowski, N., and Johns, W. R., "The Aerodynamic Instability and Disintegration of Viscous Liquid Sheets," *Chemical Engineering Science*, Vol. 18, No. 3, 1963, pp. 203–214.
https://doi.org/10.1016/0009-2509(63)85005-8
[9] Lienemann, H., Shrimpton, J., and Fernandes, E., "A Study on the Aerodynamic Instability of Attenuating Liquid Sheets," *Experiments in Fluids*, Vol. 42, No. 2, 2007, pp. 241–258.
https://doi.org/10.1007/s00348-006-0234-6
[10] Anderson, W. E., Miller, K. L., Ryan, H. M., Pal, S., and Santoro, R. J., "Effect of Periodic Atomization on Combustion Instability in Liquid-Fueled Propulsion Systems," *Journal of Propulsion and Power*, Vol. 14, No. 5, 1998, pp. 818–825.
https://doi.org/10.2514/2.5345
[11] Ahn, K., and Choi, H. S., "Combustion Dynamics of Swirl Coaxial Injectors in Fuel-Rich Combustion," *Journal of Propulsion and Power*, Vol. 28, No. 6, 2012, pp. 1359–1367.
https://doi.org/10.2514/1.B34448
[12] Wilson, M., Lineberry, D., and Moser, M., "Experimental Pulsator Characterization for Liquid Injector Research," *45th AIAA/ASME/SAE/ASEE Joint Propulsion Conference & Exhibit*, AIAA Paper 2009-5491, Aug. 2009.
https://doi.org/10.2514/6.2009-5491
[13] Fu, Q. F., Yang, L. J., and Wang, X. D., "Theoretical and Experimental Study of the Dynamics of a Liquid Swirl Injector," *Journal of Propulsion and Power*, Vol. 26, No. 1, 2010, pp. 94–101.
https://doi.org/10.2514/1.44271
[14] Khil, T., Chung, Y., Bazarov, V. G., and Yoon, Y., "Dynamic Characteristics of Simplex Swirl Injector in Low Frequency Range," *Journal of Propulsion and Power*, Vol. 28, No. 2, 2012, pp. 323–333.
https://doi.org/10.2514/1.B34169
[15] Chung, Y., Kim, H., Jeong, S., and Yoon, Y., "Dynamic Characteristics of Open-Type Swirl Injector with Varying Geometry," *Journal of Propulsion and Power*, Vol. 32, No. 3, 2016, pp. 583–591.
https://doi.org/10.2514/1.B35729
[16] Yang, A., Yang, S., Xu, Y., and Li, L., "Periodic Atomization Characteristics of Simplex Swirl Injector Induced by Klystron Effect," *Chinese Journal of Aeronautics*, Vol. 31, No. 5, 2018, pp. 1066–1074.
https://doi.org/10.1016/j.cja.2018.02.016
[17] Bazarov, V., Lee, E., Lineberry, D., Swanner, B., and Frederick, R., "Pulsator Designs for Liquid Rocket Injector Research," *43rd AIAA/ASME/SAE/ASEE Joint Propulsion Conference & Exhibit*, AIAA Paper 2007-5156, July 2007.
https://doi.org/10.2514/6.2007-5156
[18] Eberhart, C. J., and Frederick, R. A., "Fluid Oscillations of a Swirl Coaxial Injector Under High-Frequency Self-Pulsation," *Journal of Propulsion and Power*, Vol. 33, No. 4, 2017, pp. 804–814.
https://doi.org/10.2514/1.B36177
[19] Bayvel, L. P., and Orzechowski, B., *Liquid Atomization*, Taylor and Francis, Philadelphia, PA, 1993, pp. 252–266.
[20] Im, J., Kim, D., Han, P., Yoon, Y., and Bazarov, V., "Self-Pulsation Characteristics of a Gas-Liquid Swirl Coaxial Injector," *Atomization and Sprays*, Vol. 19, No. 1, 2009, pp. 57–74.
https://doi.org/10.1615/AtomizSpr.v19.i1
[21] Lefebvre, A. H., *Atomization and Sprays*, Hemisphere, New York, 1989, pp. 273–307.

G. Richards
Associate Editor